

Optical Probe and Frequency-Domain Instrumentation to Study Spatial and Temporal Correlations of Fluctuations in Tissues

M. Filiaci, V. Toronov, S. Fantini, and E. Gratton

Laboratory for Fluorescence Dynamics,
Department of Physics, University of Illinois at Urbana-Champaign,
1110 West Green Street, Urbana, Illinois 61801-3080
Phone: (217)244-5620, Fax: (217)244-7187

Abstract

We have used Photon Density Wave Fluctuation Correlation Spectroscopy (PDW-FCS) to study spatial and temporal correlations of large-scale (~ 1 mm) optical fluctuations in turbid media such as tissues. Our method uses high frequency (110 MHz) intensity modulated near-infrared light traveling in multiply scattering media. We measure the power spectra of the average value (DC), modulation amplitude (AC) and phase (Φ) of the photon density wave launched in the turbid medium. We have designed an optical probe, consisting of two source-detector pairs, which in conjunction with a correlation algorithm restricts the region probed by the photon density wave.

Key Words (170.5270) Photon density waves; (170.6510) Spectroscopy, tissue diagnostics;

1. Introduction

Biological processes related to functional activity may be characterized by fluctuations in the macroscopic optical properties of tissue. For example, brain activity changes the metabolism of a region of the brain as well as the blood flow in that region. It was demonstrated that these changes result in spatial and temporal fluctuations of tissue optical properties. In particular it was found that visual stimulation induces local changes in the optical properties of the human brain visual area [1,2].

To verify that one could observe millimeter-size optical fluctuations in turbid media and that they can be described by theory, we performed experiments with one source-detector pair. The accompanying article describes in more detail the model used in our phantom experiments [3]. Briefly, using diffusion theory and the perturbation

approach, we calculated the change in the photon density wave caused by a single, spherical, light-absorbing particle [4]. We then used two methods to verify our model: (1) fitting of time-average values of the relative change in intensity or the change in phase as a function of source-detector distance, and (2) fitting of experimental DC and phase power spectra with theoretical ones calculated from an autocorrelation function based on a 3-D flow model for the absorbing particles.

In this evaluation process we found that significant light blockage by particles coming very close to either fiber end caused a significant problem in the determination of the experimental power spectrum. With only one source-detector pair, fluctuations near either fiber end contribute much more to the relative change of the frequency-domain parameters than fluctuations deeper within the phantom or tissue (see Figure 1).

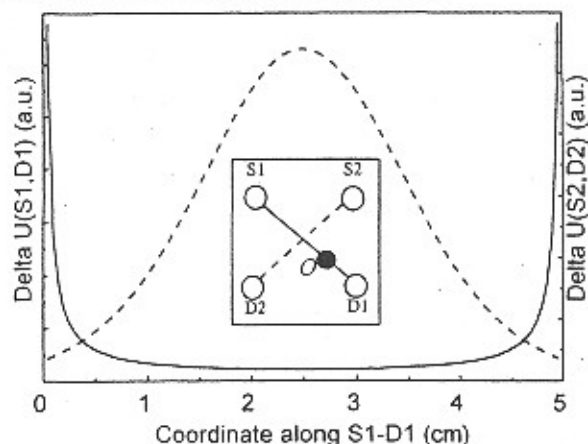


Figure 1. Change in DC of the PDW created by S_1 and S_2 (due to a small light absorbing particle O at various positions along the line connecting S_1 and D_1 , as shown in the inset), detected at D_1 (solid line) and D_2 (broken line), respectively. The line S_2 - D_2 is perpendicular to S_1 - D_1 and bisects it. The functions were calculated based on results in [5].

In the present work we propose a design for an optical probe consisting of two source-detector pairs where each source and detector is located at the corner of a square about 3 cm a side (see Figure 2). Our aim is to reduce the sensitivity to fluctuations in the superficial layers of tissue, and to better localize them in the deeper regions. To clarify the advantage of this design, suppose that the optical parameters fluctuate homogeneously in the entire region below the probe, and that fluctuations in the points separated by distances larger than Δ are uncorrelated. Consider the modulated signals U_{11} detected by detector D_1 generated by source S_1 and U_{22} detected by detector D_2 generated by source S_2 . If local fluctuations of the optical parameters are not very large, the instantaneous fluctuations of both signals are given by the integrals of the local contributions δu_{ij} over the entire region. The regions contributing most to the fluctuations of the signals U_{11} and U_{22} are defined by the light bundles around the lines S_1 - D_1 and S_2 - D_2 , respectively. Consider the cross-correlation function $\langle f_{11}(t)f_{22}(t+\tau) \rangle$, where $f_{ij}(t)$ is the DC, AC or phase of the corresponding signal. Since fluctuations in the distant regions are uncorrelated, the function $\langle f_{11}(t)f_{22}(t+\tau) \rangle$ is effectively the autocorrelation function for fluctuations in the area of characteristic size Δ located at the intersection of the light bundles for S_1 - D_1 and S_2 - D_2 . In this sense we may also consider the product of the fluctuations of two signals as a function of time, such as $\delta u_{11}(t) \times \delta u_{22}(t)$.

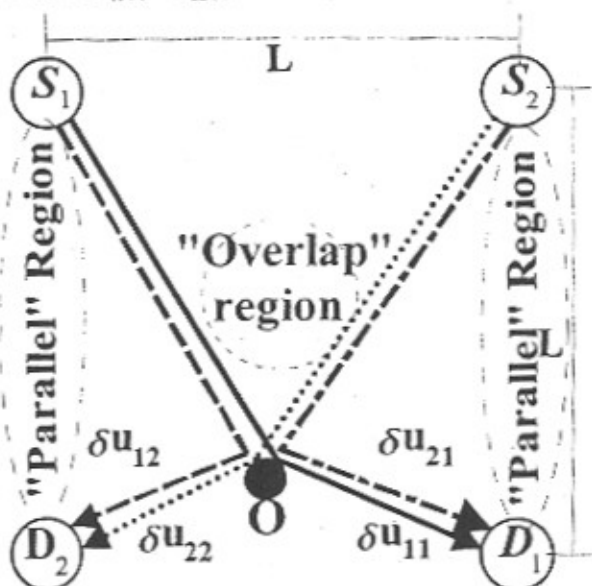


Figure 2. Optical probe consisting of two sources (S_1, S_2) and two detectors (D_1, D_2) placed at the vertices of a square of side $L=3$ cm. The photon density change caused by object O (which has different optical properties than the surrounding turbid medium) detected at detector D_j and generated by source S_i is indicated by δu_{ij} .

In addition to the signals U_{11} and U_{22} , one can also acquire the signals U_{12} and U_{21} . The correlations between U_{12} or U_{21} with U_{11} or U_{22} allow us to localize fluctuations in the two "parallel" spatial regions. The cross-correlation $\langle f_{12}(t)f_{21}(t+\tau) \rangle$ gives us information on the correlations of fluctuations between the two "parallel regions" shown in Figure 2 (this was done for the measurements on the forehead, shown in Figure 8).

2. Methods

The basic features of the frequency-domain instrument are described in the accompanying article [3] (see Figure 3). Briefly, the light source is a laser diode emitting at 750 nm, whose intensity is modulated at 110 MHz. The light is guided through a multimode silica optical fiber having a core diameter of 600 μm and a numerical aperture of 0.39. The light is collected by a glass fiber bundle (internal diameter 3.2 mm, numerical aperture 0.56) and conducted to the photomultiplier tube (PMT). The PMT voltage is modulated at 110.005 MHz, and the signal at the difference frequency is applied to the input of an interface card (ISS A2D, ISS Inc., Champaign, IL) for an IBM-PC computer, where the data processing is performed to obtain DC, AC and Φ [6].

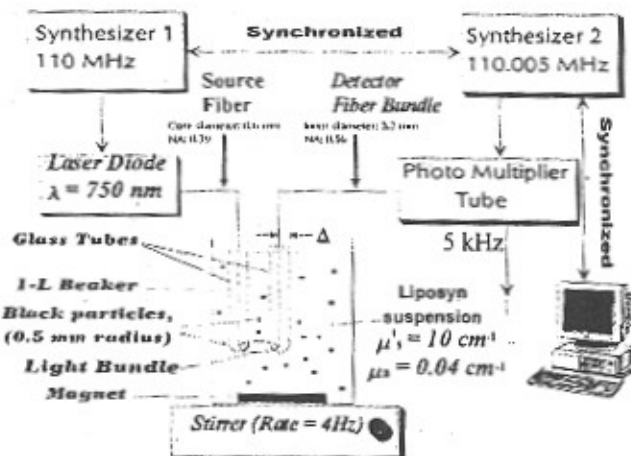


Figure 3. The PMT output at the difference frequency (5 kHz) is sent to the input of an interface card for an IBM-PC computer, where the data processing is performed to obtain the frequency domain parameters: the average value (DC), the amplitude (AC) and the phase of the signal.

When two source detector pairs were used, the two sources were multiplexed at 8 msec intervals. The time-series data acquired by the frequency domain instrument are collected into blocks of 8 seconds with a time resolution of 8 msec, or 16 msec with multiplexing (corresponding to a frequency bandwidth of 62.5 Hz and 31.25 Hz, respectively). Each 'block' is Fourier transformed. The modulus square of the transforms are

then averaged over the whole data set, to obtain the power spectrum, which in turn is the Fourier transform of the autocorrelation function of the given signal (Wiener-Khinchin theorem). If the Fourier transforms of two different signals are multiplied, then the modulus square of the result is the Fourier transform of the cross-correlation function. In the phantom experiments, relative changes of the intensity in the raw time series data for each crossed signal were multiplied to produce the product $\Delta U_{11}(t) \times \Delta U_{22}(t)$.

3. Results

3.1. Two source-detector pairs: phantom experiment

Starting with the same instrumental setup as shown in Figure 3 we added one source-detector pair (Figure 2). The two sources are rapidly turned on one at a time. A particle passing close to S_1 or D_1 will not cause a significant change in the photon density wave detected by D_2 due to S_2 (see Figure 1). Figure 4 qualitatively shows the light bundle (the volume probed by most of the photons detected) for each source-detector pair. We indicate with labels A - E some possible positions for particles that are detected in the signals shown at the top of Figure 5. The individual source-detector traces show the passage of particles in regions in which each detector responds, but as

we see in the product signal (bottom of Figure 5), positions A - C are not detected, while particles at D and E cause a significant change. A fraction of all passages occurs in the 'overlap region' of the light bundles. Figure 6 shows the

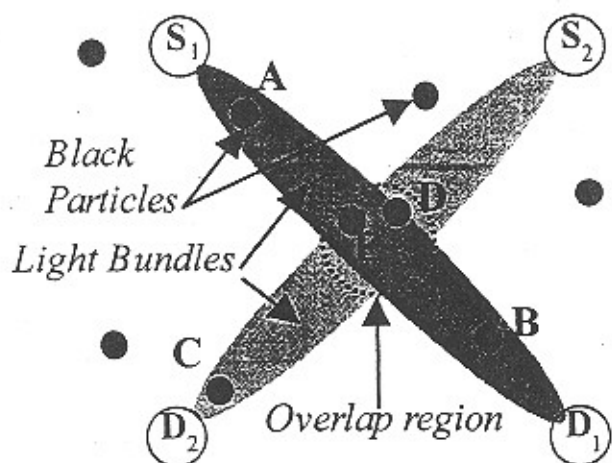


Figure 4. Light bundles for the two source-detector pairs. Possible positions of particles at times indicated by arrows in Figure 5, labeled A-E. Particles in the 'overlap region' will be detected by both source-detector pairs. The 'parallel' signals U_{21} and U_{12} may be used to determine whether particle A for example actually passed near S_1 or near D_1 .

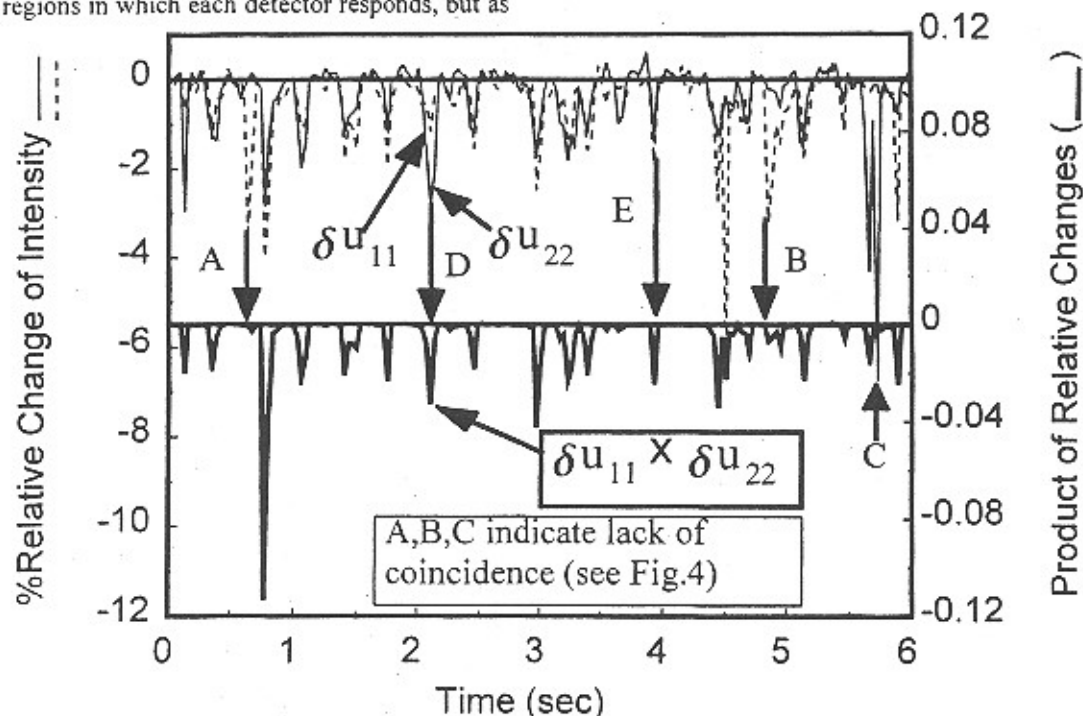


Figure 5. Time evolution of the relative DC changes in the signal of two individual source-detector pairs $\Delta U_{11}(t)$ and $\Delta U_{22}(t)$ (solid and broken lines at top), and of their product (bold line, bottom). The arrows labeled A - C indicate the individual fluctuations δu_{11} and δu_{22} at times in which a particle may have traversed an area not close to the intersection of the lines S_1 - D_1 and S_2 - D_2 . The arrows labeled D and E are times in which a particle traversed the overlap region (see Figure 4).

corresponding power spectra. The high frequency part of the cross-correlation spectrum (bold line) is smaller than the same part of the spectrum of each individual detector, as evident in the log-scale plot. This may be explained by particles coming close to either source or detector creating more rapid changes in the PDW than those passing in the overlap region.

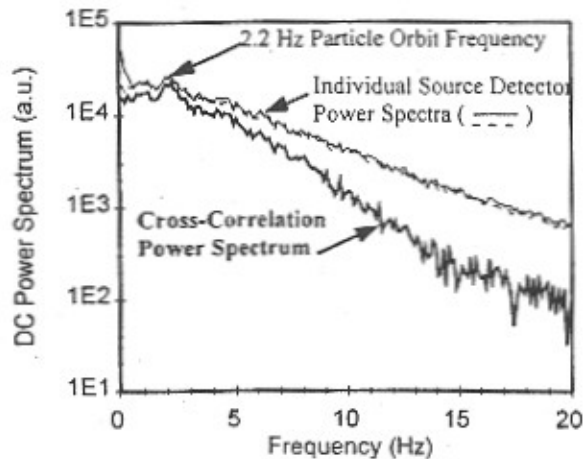


Figure 6. DC power spectra of the individual source-detector pairs and their cross-correlation.

3.2. Simultaneous measurement at two points on the forehead

We placed two source-detector pairs 6 cm apart on a subject's forehead, to prevent cross-talk between the two detectors (this is a two source-detector pair probe in which only the parallel signals are considered). The power spectra show the normal heart beat components, as does the cross-correlation spectrum (Figure 7). The *coherence spectrum* (defined as the ratio

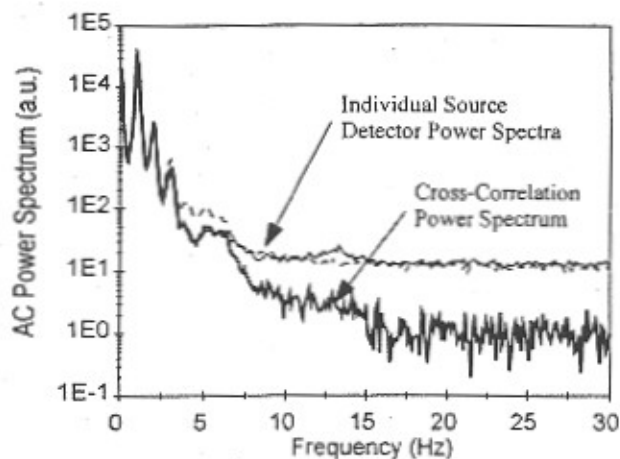


Figure 7. AC power spectra of two source-detector pairs (solid and broken lines) positioned 6 cm apart on the forehead. The cross-correlation spectrum (bold line) is very similar to each individual one, but the baseline is approximately one-tenth the value for the individual pairs.

of the modulus of the cross-correlation spectrum to the square-root of the product of the power spectra of 2 signals) shows significant coherence up to about 8 Hz, along with a non-zero phase lag (Figure 8). The phase of the two signals becomes random when they lack coherence.

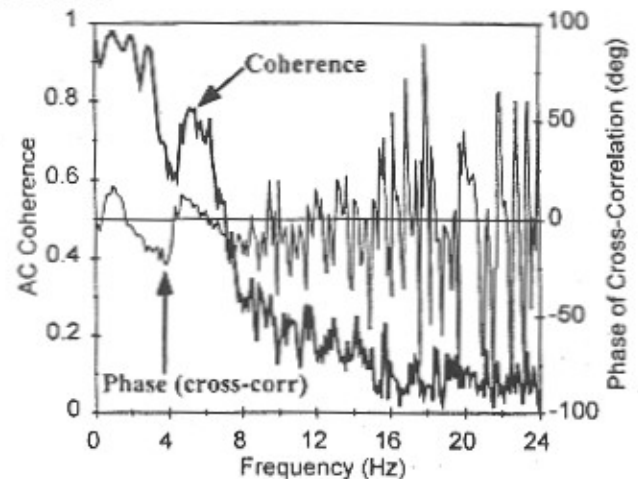


Figure 8. AC coherence spectrum of the two signals detected on the forehead. The phase between the two signals is measurable and non-zero when the two signals exhibit coherence. The peaks in the coherence are due to the heart beat and harmonics. The phase changes of the signals are as yet unexplained.

4. Conclusions

Our instrument is able to detect large-scale (~mm) optical fluctuations *in vitro*, and studies *in vitro* confirm that optical fluctuations can be detected over a bandwidth of ~100 Hz. We were able to detect fluctuations *in vivo* in studies of the brain. The optical probe consisting of two crossed source-detectors reduces sensitivity to optical fluctuations near the surface, making it more suitable for *in vivo* applications. The analysis of the four signals U_{11} , U_{21} , U_{12} and U_{22} allow localization of the fluctuations within deeper regions of the tissue.

5. Acknowledgements

This work was supported by NIH grants RR03155 and CA57032

6. References

- [1] G. Gratton, P.M. Corballis, E. Cho, M. Fabiani, and D.C. Hood, "Shades of Gray Matter: Noninvasive Optical Images of Human Brain Responses During Visual Stimulation," *Psychophysiology* 32, 505-509 (1995)
- [2] R. Wenzel, H. Obrig, J. Ruben, K. Villringer, A. Thiel, J. Bernardin, U. Dirnagl, and A. Villringer, "Cerebral Blood Oxygenation Changes Induced by

- Visual Stimulation in Humans," *J. Biomed. Optics* **1**, 399-404 (1996)
- [3] V. Toronov, M. Filiaci, S. Fantini, and E. Gratton, "Study of Large Scale Fluctuations in Turbid Media by Photon-Density-Wave Fluctuation Correlation Spectroscopy," in this issue
- [4] D.A. Boas, M.A. O'Leary, B. Chance, and A.G. Yodh, "Scattering of Diffuse Photon Density Waves by Spherical Inhomogeneities within Turbid Media: Analytic Solution and Applications," *Proc. Natl. Acad. Sci. USA* **91**, 4887-4891 (1994)
- [5] V. Toronov, M. Filiaci, S. Fantini, and E. Gratton, "Photon Density Wave Correlation Spectroscopy Detects Large-Scale Fluctuations in Turbid Media," *Physical Review E* (submitted, Dec. 1997)
- [6] B.A. Feddersen, D.W. Piston, and E. Gratton, "Digital Parallel Acquisition in Frequency Domain Fluorimetry," *Rev. Sci. Instr.* **60**, 2929-2936 (1989)